Podcasts

Modeling regional aboveground carbon stock dynamics affected by land use and land cover changes

A.D. Malik[1,*], M.C.W. Arief[2], S. Withaningsih[3], P. Parikesit[4]

[1]Center for Environment and Sustainability Science, Universitas Padjadjaran, Bandung, West Java, Indonesia

[2] Department of Fisheries, Faculty of Fisheries and Marine Science, Universitas Padjadjaran, Sumedang, West Java, Indonesia

[3] Sustainability Science Masters Study Program, Graduate School, Universitas Padjadjaran, West Java, Indonesia

[4] Department of Biology, Faculty of Mathematics and Natural Sciences, Universitas Padjadjaran, Sumedang, West Java, Indonesia

ARTICLE INFO

ABSTRACT

BACKGROUND AND OBJECTIVES: Land use and land cover changes are affected by massive construction, urban expansion, and exploitative agricultural management. These pressures threaten the potential of aboveground carbon storage in Rancakalong District, West Java, Indonesia. In that massive construction and agricultural expansion are ongoing, it is critical to detect the potential changes in carbon stocks in the region. This study evaluated the impact of land use and land cover changes on aboveground carbon stock potential in Rancakalong District, West Java, Indonesia, by incorporating several ground-based carbon inventories into geographic information systems and remote sensing approaches. The spatiotemporal dynamics of the aboveground carbon stocks were assessed using Integrated Valuation of Ecosystem Services and Tradeoffs models.
METHODS: Aboveground carbon stocks were estimated using the integrated approach of field inventory and geographic information systems. Land use and land cover changes were assessed from remotely sensed imagery data recorded in 2009 and 2021 using the maximum likelihood classification method in the geographic information as a collection of layers and other elements in a map 10.6 package. Tree height and diameter were collected within the purposively distributed plots with a size of 30 × 30 square meters. Vegetation biomass was assessed using an allometric equation, and aboveground carbon stock data were extrapolated to the landscape scale using a linear regression model of measured carbon stocks and the Normalized Difference Vegetation Index derived from recent satellite imagery.
FINDINGS: Vegetated areas were predominant in 2009 and 2021. Vegetation covered 51 percent of the total area in 2009, increasing to 57 percent in 2021. Regarding agricultural area, mixed gardens and drylands decreased between 2009 and 2021. Meanwhile, paddy fields were the only agricultural land use to increase between 2009 and 2021. The bare land and built-up expansion related to the observed land clearing for the Cisumdawu Highway mainly came from the conversion of mixed gardens, paddy fields, and drylands. The results show that the land use and land cover changes in Rancakalong District have caused a reduction in aboveground carbon stocks by 11,096 tons between 2009 and 2021. The highest reduction in aboveground carbon stocks occurred in mixed gardens, while a slight increase in aboveground carbon stocks occurred in forests, shrubs, and paddy fields. The results highlight the contribution of mixed gardens to carbon storage as they are visually similar to forests in the structure and composition of vegetation.
CONCLUSION: Land use and land cover changes directly affected the aboveground carbon stock potential in Rancakalong District, indicated by an 11,096-ton reduction in the stocks. This shortage of carbon stock potential was mainly attributed to the massive reduction in mixed garden areas between 2009 and 2021 by 12 percent, which caused a significant decrease in aboveground carbon stocks. The application of the Integrated Valuation of Ecosystem Services and Tradeoffs model is efficient in analyzing the effect of land use and land cover change on aboveground carbon stock dynamics and can be widely used in environmental engineering studies involving remote sensing approaches.

NUMBER OF REFERENCES
88

NUMBER OF FIGURES
6

NUMBER OF TABLES
3

*Corresponding Author:
Email: annas12001@mail.unpad.ac.id
Phone: +6283 8265 60209
ORCID: 0000-0003-0588-387X

INTRODUCTION

Climate change and global warming have become major threats to global ecosystems (Hassan and Nile, 2021; Frimawaty *et al.,* 2023; Arredondo Trapero *et al.,* 2023). The recent increase in greenhouse gas emissions that has resulted from massive human social development and industrialization is one of the main causes of climate change (Javaherian *et al.,* 2021). Temperatures in places inhabited by more than one-fifth of humanity have already risen by 1.5 degrees Celsius (C) over preindustrial levels in at least one season (Javaherian *et al.,* 2021). Without mitigation efforts to reduce greenhouse gases, the global temperature is expected to continue to rise in the 21st century, ranging from a median increase of 3.7°C to 4.8°C (IPCC, 2014).

The primary factors causing climate change are thought to be carbon emissions and greenhouse gases, and their levels continue to meet the upper limit of the model scenario developed by the IPCC (Jagdish *et al.,* 2013). As a consequence of landscape modification, land use and land cover (LULC) change impacts the ability of a landscape to reduce carbon emissions. LULC changes further impact the distribution of soil organic matter as an area shrinks over time (Zhao *et al.,* 2018; Karbassi *et al.,* 2015). Moreover, modifications in LULC exert increasing pressure on regulatory ecosystem services such as carbon sequestration (Solomon *et al.,* 2018). The benefits humans gain from ecosystems are referred to as "ecosystem services" (Millennium Ecosystem Assessment, 2005). All ecosystem services are needed for human survival and livelihoods (Solomon *et al.,* 2017). The regulation of gas concentrations that circulate between the ecosystem and atmosphere of the earth and have an impact on the world's climate is carbon sequestration (Lee *et al.,* 2022). The dynamics of the carbon cycle are affected by LULC changes, which affect emission rates and carbon sequestration (Coutinho *et al.,* 2015). The ability of terrestrial carbon pools may also be disturbed by these impacts, which can affect the accumulation of many sources of carbon (Zhao *et al.,* 2018). Terrestrial ecosystems play an essential role in carbon sequestration. According to the FAO (2016), carbon sequestered in above- and belowground biomass is estimated at approximately 296 gigatons (Gt) and 44% is stored in plant biomass. Conversely, the emission of carbon dioxide (CO_2)

resulting from vegetation biomass deterioration was estimated at 12.5% of the total CO_2 emissions (Masripatin *et al.,* 2010). Aboveground biomass consists of all living things and vegetation that exists in terrestrial ecosystems, such as trees, shrubs, and herbaceous plants (Piyathilake *et al.,* 2022). According to a report from the Forest Resource Assessment, the world's carbon stored in forest biomass was 289 Gt (Ostadhashemi *et al.,* 2014). The carbon stocks in natural forests are believed to be one of the most vital ecosystems for combating anthropogenic climate change (Thom *et al.,* 2017). Forest areas have ten times greater potential for carbon stocks than other types of vegetation; however, many forests are currently being deforested (Masripatin *et al.,* 2010). Changes in forest cover and other land use with carbon sequestration potential influence carbon dynamics (Dida *et al.,* 2021). Between 2005 and 2010, the carbon contained in the world's forest biomass was expected to decrease by 0.5 Gt each year. This reduction was primarily due to a decrease in worldwide forest area (Forestry Economics and Policy Division, 2010). Likewise, between 2015 and 2016, it was estimated that forests in Indonesia experienced 0.63 million hectares (ha) of deforestation (KLHK, 2018). Most carbon emissions come from the coal energy sector, and this rate is predicted to increase further until reaching 434.96 parts per million (ppm) in 2050, where carbon increases that exceed 400 ppm can be categorized as a global phenomenon (Cahyono *et al.,* 2022). In this context, investigating the potential loss of valuable ecosystem components as a result of LULC change is essential (Lahiji *et al.,* 2020). Numerous studies in Indonesia have analyzed the potential of various ecosystems to sequester carbon, for example, in state forests (Darmawan *et al.,* 2022), production forests (Situmorang *et al.,* 2016), urban green spaces (Dewanto and Jatmiko, 2021), mangroves (Kusumaningtyas *et al.,* 2022), and agroforestry systems (Latifah *et al.,* 2018). However, limited studies have discussed how LULC changes impact ecosystem services, and a spatiotemporal model of carbon stock dynamics has not been produced. The recent rapid development of geographic information systems (GIS) provides an opportunity to identify LULC changes over time and comprehensively detect disturbances in a particular ecosystem service (Zhao *et al.,* 2019). Furthermore,

a spatial model provides a clearer explanation of how disturbance impacts ecosystem services (Jiang *et al.,* 2021). The study of LULC changes and measurement of the aboveground carbon stock may vary using remote sensing and GIS. Several previous studies have focused on revealing the significant effects of LULC changes on carbon stocks using GIS and remote sensing approaches. A typical simulation model for carbon stock dynamics incorporating annual maps was performed to analyze the effect of LULC changes on vegetation biomass and carbon stocks (Liu *et al.*, 2016). The assessment of LULC changes and vegetated aboveground carbon stocks using multispectral data in remote-sensing-based methodology revealed a relevant decrease in vegetated areas (Massetti and Gil, 2020). Another study conducted by Piyathilake *et al.* (2021) used the GIS approach and InVEST model to predict the LULC type containing the largest carbon stocks on a regional scale. Later, the use carbon budget model, which focuses on the prediction of carbon dynamics affected by several disturbances and LULC variations, was performed by (Tang *et al.* 2022). The empirical model also incorporates some ecological processes regarding the plant species' traits and characteristics and climate data. However, these studies used secondary data, such as available vegetation maps, geodatabase of vegetation stand attributes, and national statistics data of biomass growth to obtain carbon stocks. Detailed information regarding the combination of remote sensing and integrated field surveys at the regional scale remains limited. In this study, rather than relying only on carbon data sources from published studies and reports, the integration of a few field carbon inventory data points with GIS and remote sensing methods is expected to obtain more accurate and precise carbon estimation results. The normalized difference vegetation index (NDVI) is a metric derived from remotely sensed images that is commonly used in predicting biophysical factors, such as aboveground biomass and carbon (Wani *et al.,* 2021). Typically, some parametric models have been applied to discover the direct relationship between aboveground biomass and metrics/spectral values derived from satellite imagery (Vafaei *et al.,* 2018; Zhu and Liu, 2015). Several spatially based decision models for ecosystem services assessment have

been widely applied (Bagstad *et al.,* 2013), one of which is Integrated Valuation of Ecosystem Services and Tradeoffs (InVEST) (Sharp *et al.,* 2020). InVEST is a distinguished model that has been widely applied to assess global ecosystem services (Piyathilake *et al.,* 2022). The advantages of this model include its low data requirements and ease of use (Cong *et al.,* 2020). Models for regulatory ecosystem services have been commonly applied in InVEST, and the model has been used to assess carbon sequestration under multiple scenarios (Posner *et al.,* 2016). The InVEST model uses LULC projection maps and quantitative data on ecosystem services (Nelson *et al.,* 2009). The model needs an estimation of the carbon stocks in at least one of the four carbon pools for each LULC map. These data can be used to create a projection model of the amount of carbon stored in a class of land cover over time and predict carbon sequestration (Sharp *et al.,* 2018). This study employs the aboveground biomass of vegetation as it is the most active carbon pool in the carbon cycle (Harper *et al.,* 2018). Land deterioration has occurred in Sumedang Regency, West Java, Indonesia. According to Khaerani *et al.* (2018), a protected forest and production forest conversion of 7,817 ha between 2015 and 2017 violated the regional planning for the Sumedang Regency. In recent years, forest cover degradation has been affected by the megaproject in Sumedang Regency. They are the Cisumdawu Highway project, which connects Bandung, the capital city of West Java, with Kertajati International Airport, and the Jatigede Hydropower Plant, which is expected to generate 2 × 25 megawatts (MW) of electricity. As a result of this forest cover degradation, carbon sequestration has likely been significantly diminished. Rancakalong is a district in Sumedang Regency. Segments of the Cisumdawu Highway also pass through this District, resulting in LULC change. Since these massive constructions are ongoing, determining the link between LULC change and carbon stocks in this area is critical, as various LULC classes have varying effects on carbon stocks (Toru and Kibret, 2019). The aim of this study is to analyze spatial and temporal dynamics of aboveground carbon stocks associated with LULC change in Rancakalong using the InVEST model. This study was conducted in Rancakalong District, which is situated in Sumedang Regency, West Java Province, Indonesia in 2009 and 2021.
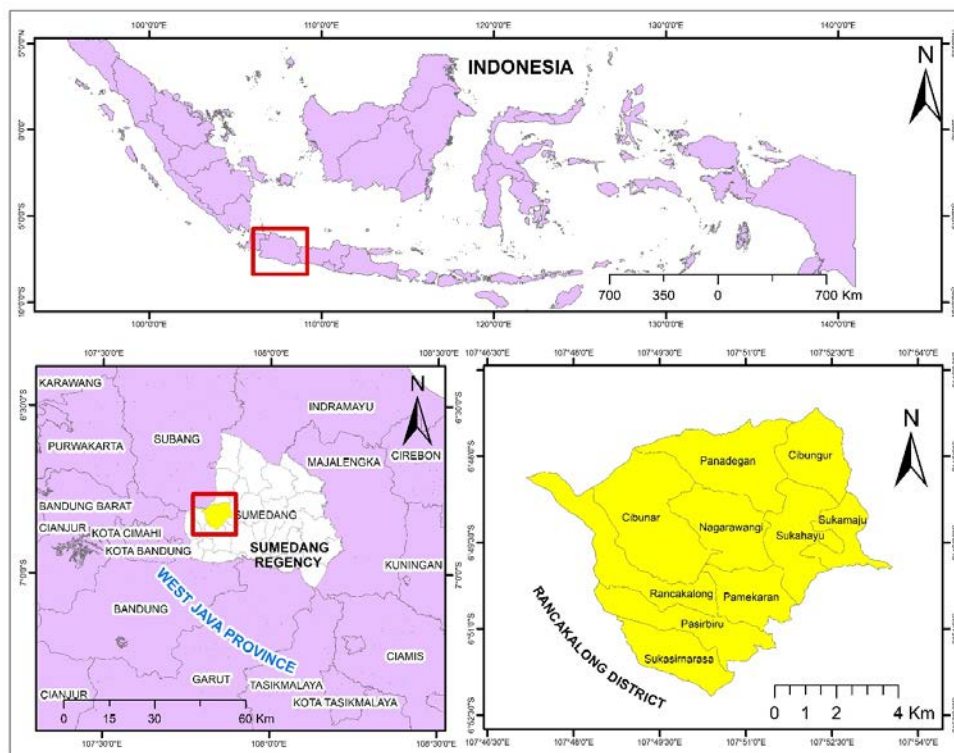
Fig. 1: Geographic location of the study area in Rancakalong District, Indonesia

MATERIALS AND METHODS

Research site

Rancakalong District is located in the western part of Sumedang Regency 16 kilometers (km) from the capital of Sumedang Regency, West Java Province, Indonesia (Fig. 1). The mean temperature in the study area is 24.7°C, and the mean precipitation is 2570 millimeters per year (mm/y) (Sampurno and Thoriq, 2016). The total area of Rancakalong District is 5574.12 ha, dominated by hills and mountainous landscapes, and the elevation ranges from 500 to 1500 meters (m) above sea level (Sumedang Regency, 2019). The geographic conditions indicated that large parts of the area are barely accessible. Most of Rancakalong's people are working in the agricultural sector, reflected by the agriculture area as the major land use in Rancakalong, with the characteristics of upland agricultural systems and paddy fields reaching 3383.77 ha or 60.71 percent (%) of the Rancakalong District (Sumedang Regency, 2019). The forests lie on the very steep slope hillside of Cibunar Mountain and cover 146.29 ha of the area. In recent days, the Rancakalong area has been exposed to environmental pressure from the development of the Cisumdawu Highway as segments of the toll road pass through the area and have affected massive LULC changes.

Data collection and sampling design

The magnitude of the data collected was at the Rancakalong District scale as part of the Sumedang Regency. The integrated approach combining the direct measurement of carbon stocks and spatial analysis was conducted to assemble the required primary and secondary data. The primary data of the carbon stocks collected by direct measurement of aboveground biomass of the vegetation stands measures the diameter at breast height (DBH) and height. Most of the area was difficult to access due to very steep slopes around the hills and mountains and the high rainfall that occurred during the research. The vegetation stands were sampled in the study area and quantified using a purposive sampling technique considering safety, climate, and topographic factors. The sample plot size of 30 × 30 square meters (m²)

refers to the pixel size of medium-resolution remotely sensed satellite imagery (~30 m). The secondary data contain the global spatial distribution of crop yield data in tons/hectare (tons/ha) for all commodities in Rancakalong (rice, sweet potato, maize, groundnut, banana, and cassava), which can be considered biomass in tons/ha and tree density of all measured trees. The crop yield information was collected from the Global Agroecological Zones+ (GAEZ+) (Frolking *et al.,* 2020) data on global gridded crop harvest areas, crop production, and crop yields. Tree density was obtained from the global wood density database (Zanne *et al.,* 2009). Furthermore, the secondary data of the multispectral image of Landsat 5 Thematic Mapper (TM) recorded on 3 May 2009 and Landsat 8 Operational Land Imager (OLI) recorded on 16 September 2021 were used as spatial data for InVEST modeling.

Preprocessing

Satellite imagery pre-analysis was required to correct the atmospheric disturbance of the multispectral image data. This process corrected the pixel value of the image data and allowed the pixel value to depict the true condition of the terrestrial ecosystem. Without this correction, the image sensor may have failed to absorb the object's reflection of the earth due to atmospheric disturbance. The preprocessing step consisted of radiometric calibration and atmospheric correction. Before calibration, the satellite images were cropped to the area of interest. Next, the vector administrative boundary of Rancakalong District was selected as the masking area. In radiometric calibration, the multispectral image data, or so-called digital numbers (DN), were converted into the top of atmosphere (TOA) radiance and reflectance by rescaling the DN values in the metadata text file extension (MTL). This process is a prerequisite for DN value conversion into a surface reflectance value when correcting for atmospheric disturbance (Chavez, 1989). This reflectance measurement produces a vegetation index of the imagery data (Jaya *et al.,* 2022). To generate the TOA radiance value, the radiance rescaling factors of the MTL were used and included in Eq. 1 (Hua and Ping, 2018).

$$L_\lambda = M_L Q_{cal} + A_L \tag{1}$$

where:
L_λ = TOA spectral radiance
M_L = The MTL-derived multiplicative rescaling factor
A_L = MTL's additive rescaling factor
Q_{cal} = Standard product pixel values or DN value of a specific pixel

The following stage involved converting TOA spectral radiance to TOA reflectance. The images in spectral radiance were converted to reduce the in-between-scene variability through normalization for solar irradiance (Chander and Markham, 2003). This step is imperative to cross-calibrate all Landsat sensors (Li *et al.,* 2018). For the Landsat 5 TM, the spectral radiance ($L_\ddot{e}$) was converted to the surface and atmospheric reflectance using Eq. 2 (Chander and Markham, 2003).

$$\rho_p = (\pi L_\lambda d^2) / (ESUN_\lambda \cos\Theta_s) \tag{2}$$

where:
ρ_p = Planetary reflectance
π = phi
L_λ = TOA spectral radiance
d = The astronomic distance between Earth and Sun
$ESUN_\ddot{e}$ = The mean value of solar exoatmospheric irradiances
Θ_s = Angle of the sun's zenith in degrees (90° − solar elevation)

Meanwhile, all rescaling factors for Landsat 8 OLI imagery were found in the MTL, meaning that the conversion to TOA radiance was unnecessary. The conversion was conducted using Eq. 3 (Nijhawan and Jain, 2018).

$$\rho\lambda' = M_\rho Q_{cal} + A_\rho \tag{3}$$

where:
$\rho\lambda'$ = TOA reflectance, in which the sun's angle correction is not necessary for OLI
M_ρ = MTL-derived band-specific multiplicative rescaling factor
A_ρ = Additive rescaling factor from the MTL for each band
Q_{cal} = Standard product pixel values or DN value of a specific pixel

The effects of atmospheric scattering should be considered when measuring reflectance at the

ground, also known as surface reflectance (Chavez, 1989). The surface reflectance is applied using Eq. 4 (Moran *et al.,* 1992).

$$\rho = \left[\pi *(L_\lambda - L_p)*d^2 \right] / [T_v *((ESUN_\lambda *cos\Theta_s * T_z) + E_{down}] \quad (4)$$

where:

ρ_λ = Surface reflectance
π = phi
L_λ = TOA spectral radiance
L_p = Path radiance
d = The astronomic distance between Earth and Sun
T_v = Atmospheric transmittance in the viewing direction
Θ_s = Solar zenith angle in degrees (90° − solar elevation)
T_z = Atmospheric transmittance in the illumination direction
$ESUN_\lambda$ = The mean value of solar exoatmospheric irradiances (ESUN is not required for Landsat 8 OLI bands)
E_{down} = The downwelling diffuse irradiance

All preprocessing steps were run in the Semiautomatic Classification Plugin (SCP) integrated into the QGIS 3.16 software. The SCP is a free plugin for QGIS that facilitates satellite image conversion to reflectance to generate the best condition of the Earth's surface by reducing the atmospheric condition. As the final step of preprocessing (atmospheric correction/surface reflectance), dark object subtraction 1 (DOS1) atmospheric correction was applied in the plugin.

LULC classification

LULC classification was applied to both Landsat 5 TM and Landsat 8 OLI images. This process produces raster data of LULC classes and later will serve as the data for InVEST modeling. All raster images were stacked or composited to produce a single raster and multispectral image. Since a pansharpened raster band is available in the multispectral image of Landsat 8 OLI, an image enhancement tool was used to sharpen the image resolution and clarify the image during the remote sensing process. The image classification process using maximum likelihood classification (MLC) was run in the geographic information as a collection of layers and other elements in a map.

(ArcMap) 10.6. Numbers of training samples were drawn on each satellite image representing the LULC classes (forests, mixed gardens, paddy fields, shrubs, built-up land, drylands, and bare land). This nomenclature variation of LULC classes was selected following guidance from the Ministry of Forestry and Environment of Indonesia and the Regional Planning Agency of Sumedang regarding the remote sensing method for medium-resolution satellite imagery data. The supervised technique identifies and classifies the pixel values drawn in the training sample with other identical pixel values. Visual interpretation of the satellite imagery was assisted by high-resolution Google Earth imagery and ground-truthing at the study site. The determination of selected variations of LULC classes was also helped by the Google Earth imagery and ground-truthing approach. The best band combination for built-up area classification is the natural color band combination, that is, band 4-3-2 for Landsat 8 OLI and band 3-2-1 for Landsat 5 TM (Liu *et al.,* 2018). Conversely, the false color band combination is the most suitable for vegetation mapping, namely, band 5-4-3 for Landsat 8 OLI and band 4-3-2 for Landsat 5 TM (Liu *et al.,* 2018). The false color band is superior because tree leaves have a large amount of chlorophyll, which can better absorb red light from the infrared spectrum (Zhang *et al.,* 2012). Later, an accuracy assessment was conducted to minimize LULC classification errors due to the sampling technique and the potential for misinterpretation of pixel values in the imagery data. The assessment employed a matrix of the error to identify pixel misclassification (Yesserie, 2009). The Kappa coefficient is an appropriate analysis for nominal data image classification models that partially rely on ground-truth data (Senseman *et al.,* 1995).

Vegetation index identification

A vegetation index distribution map was produced to extrapolate the direct biomass and carbon stock measurements of vegetation stands from the plot scale to the landscape scale. This index was also useful to identify the index value of the vegetation present in the study site. The most commonly used spectral vegetation index is NDVI. To identify the current state of vegetation in the study area, the multispectral image data were converted into a raster map containing the values of the vegetation

index. In this study, NDVI provided information about the canopy and vegetation coverage and depicted this information in a vegetation distribution map (Calderón-Contreras and Quiroz-Rosas, 2017). According to Marchetti *et al.* (2016), NDVI patterns can map the physiognomy and elevation of various vegetation types. This process permits mapping of different areas covered by vegetation (e.g., forests, mixed gardens, shrubs, and paddy fields). In this study, the Landsat 8 OLI recorded on 16 September 2021 was used to obtain the NDVI. The NDVI of the multispectral image is a division between the near-infrared and red bands, which in Landsat 8 OLI is related to Bands 5 and 4. The NDVI used to identify the difference in vegetation quality was obtained using Eq. 5 (Rouse *et al.,* 1974).

$$NDVI = \frac{NIR\text{-}Red}{NIR\text{+}Red} \tag{5}$$

where:
NDVI = Normalized Difference Vegetation Index
NIR = Near-infrared band (Band 5)
Red Band = Red band (Band 4)

The NDVI produces a value between –1.0 and 1.0, where negative values represent water bodies or bare lands and higher positive values indicate dense vegetation (Calderón-Contreras and Quiroz-Rosas, 2017). Such higher values are is due to dense vegetation's capacity to absorb much of the red spectrum while reflecting much of the near-infrared (Davies *et al.,* 2016). The higher the value of the NDVI, the higher the photosynthetic activity of a particular identified area of vegetation (Jamali *et al.,* 2011).

Biomass and Carbon Stock Measurement
The sampling technique considered the spatial distribution of each NDVI class. The sample was ensured to represent each class of NDVI. Deforestation was heavily affected by LULC changes; therefore, only the aboveground biomass of vegetation was measured. In the sample plots, the name of the species, DBH, and the height of the trees were measured. The estimation of biomass was conducted using Eq. 6. This allometric equation and coefficient are suitable for aboveground biomass estimation in most tropical moist regional locations, considering DBH, wood density (ρ), and tree height (T) as the most important predictive variables (Chave *et al.,* 2005).

$$AGB = 0.0509 * \rho * DBH^2 * T \tag{6}$$

where:
AGB = Total aboveground biomass (kg)
DBH = Diameter at breast height (~1.3 m)
ρ = Wood density (gr/cm³)
T = tree height (m)

The biomass carbon content was calculated by multiplying the biomass estimation result with a default value of 46% (Hairiah *et al.,* 2011). Carbon stocks obtained from field measurements were extrapolated to the landscape scale using correlation analysis. A single explanatory variable regression was selected to identify the correlation between NDVI values and the field measurement of carbon stocks (Batsaikhan *et al.,* 2020). In the regression model, the dependent variable (Y) was the plot-level carbon stock measurement result, and the independent variable (X) was the NDVI value distribution map. A scatterplot of NDVI values was produced, and the carbon stock was measured in all permanent plots to ensure that the distribution of plot carbon data matched the trend of the NDVI (Basalumi *et al.,* 2018). The correlation analysis was performed in IBM SPSS Statistics 26 software. To confirm that the study area's real carbon stocks could be modeled by the simple linear regression equation, a standard error of estimate (SEE) accuracy test was conducted on the result of the obtained carbon model and compared with the actual field carbon data in all permanent plots. The SEE analysis was calculated using Eq. 7 (Smith, 2015).

$$SEE = \sqrt{\frac{\sum_{i=1}^{n}\left(y_i - \widehat{y_i}\right)^2}{n - 2}} \tag{7}$$

where:
SEE = Standard Errors of Estimate (tons/pixel)
$\sum_{i=1}^{n}\left(y_i - \widehat{y_i}\right)^2$ = Difference value between the carbon model and actual field carbon stocks
n = number of plots

The carbon stocks model was extrapolated from the plots to the landscape scale by the Raster Calculation feature in QGIS 3.6 software. This process produced the final carbon model distribution map in a raster image format.

InVEST carbon storage model

A product of the Natural Capital Project, the InVEST Carbon Storage and Sequestration Model is software for ecosystem services mapping and calculation. In this study, InVEST was used to model the carbon stock dynamics in the study site. Specifically, the results of the older carbon stocks spatial model were compared with the more recent model. InVEST carbon modeling requires maps of LULC classification and carbon stock data in tons/ha. This study uses aboveground biomass as the only carbon pool. The model produces both numeric and spatial data in a raster output for further GIS analysis and decision-making processes (Shrestha *et al.,* 2021). The LULC raster data, which are necessary for the carbon storage model, were obtained from the LULC image classifications from 2009 and 2021. The LULC classifications contained attribute tables with information on LULC classes (forests, mixed gardens, paddy fields, shrubs, built-up land, dryland, and bare land). The result of the carbon stock estimation spatial data from the previous extrapolation process was converted into numeric values of carbon density for each LULC class. Carbon density values were then aggregated in a comma-separated value (csv) file format. All LULC raster images and the .csv file were integrated into the InVEST software to begin modeling the current aboveground carbon storage. The final result

contained carbon storage distribution maps in a temporary instruction file format (tiff).

RESULTS AND DISCUSSION

Land use and land cover changes

As shown in Fig. 2, the classification identified LULC changes in the Rancakalong District. A seen in Table 1, the largest LULC class area in both 2009 and 2021 was mixed gardens. In 2009, mixed gardens (31%) were followed by drylands (21% as the second most common class). Meanwhile, mixed gardens (25%) and paddy fields (13%) were the most common LULC classes in 2021. According to LULC change detection, the area of mixed gardens and drylands decreased between 2009 and 2021 by 6% and 8%, respectively. The areas of shrubs, forests, paddy fields, and bare land increased by 9%, 2%, 2%, and 2%, respectively. The supervised classification detected that vegetated land was predominant in 2009 and 2021. In this study, forests, mixed gardens, and shrubs were considered to be vegetated areas, as vegetation cover was predominant in each area. Vegetation covered 51% of the total area in 2009. In 2021, the vegetated area covered 57% of the total area, indicating a 6% increase in vegetated areas. This increase was driven by shrubs, as this type of vegetation expanded 10% between 2009 and 2021.

At the LULC level, the conversions occurred at
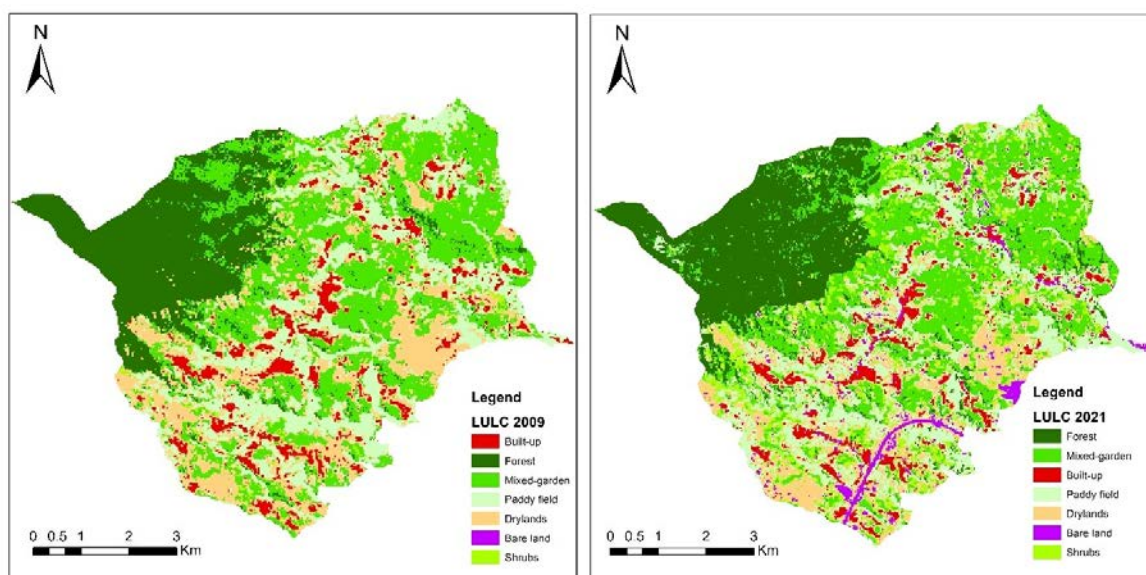
Fig. 2: Map of LULC classification in Rancakalong District in 2009 and 2021

different rates depending on the type of LULC class (Table 2). For example, forests were mostly converted to mixed gardens (12%), followed by these areas' conversion to paddy fields (3%) and shrubs (2%). Mixed gardens—the most common LULC class in the study site—experienced a 12% conversion to forests, followed by conversion to shrubs (13%) and paddy fields (11%). The estimated conversions between forests and mixed gardens may have been biased by the visual characteristics of these LULC classes potentially leading to misclassification. According to the remote sensing method, forests and mixed gardens are visually similar since the mixed garden in the study area can be considered an agroforestry system managed by local communities that take part as forest buffer areas. As agriculture is the main occupation of Rancakalong District's people, the conversion of forests and mixed gardens to paddy fields was mainly attributed to these areas expanding to fulfill the needs of Rancakalong's people for this type of agricultural system.

The increase in forest cover can be largely attributed to the rise in mixed gardens because mature mixed gardens are visually similar to forest cover and are both dominated by perennial plants. In contrast, the mixed garden area decreased between 2009 and 2021. The mixed gardens were mostly converted into shrubs, indicating some abandonment of mixed gardens following plant-clearance activities by farmers. Paddy fields were the only agricultural land use to become more prevalent, increasing from 20% to 22% between 2009 and 2021 (Table 1). Meanwhile, the other agricultural areas, mixed gardens, and drylands, decreased between 2009 and 2021. As in the nonvegetated and non-agricultural areas, the newly built-up areas largely resulted from the conversion of drylands (6%) and paddy fields (2%) (Table 2). The largest bare land conversion came from paddy fields (4%), followed by drylands (3%) (Table 2). The bare land conversion was related to the observed land-clearing activities for the Cisumdawu Highway project, which started

Table 1: Estimated area for each LULC class in 2009 and 2021

LULC classes	2009 (ha)	2021 (ha)	2009 (%)	2021 (%)	Area change (%)
Drylands	1150.17	712.90	21%	13%	−8%
Forests	1134.54	1218.73	20%	22%	2%
Mixed gardens	1736.90	1413.36	31%	25%	−6%
Bare land	0.18	138.70	0%	2%	2%
Built−up	342.10	286.61	6%	5%	−1%
Paddy fields	1130.93	1245.90	20%	22%	2%
Shrubs	57.59	536.22	1%	10%	9%
Total	5552.41	5552.41	100%	100%	

Table 2: Conversion area matrix of LULC classes between 2009 and 2021

	LULC	2021 ha (%)						
		Drylands	Forests	Mixed gardens	Bare land	Built-up	Paddy fields	Shrubs
2009 ha (%)	Drylands	372.39 (32%)	30.13 (3%)	149.87 (13%)	35.78 (3%)	65.29 (6%)	315.09 (−27%)	181.61 (16%)
	Forests	8.7 (−1%)	928.50 (82%)	134.10 (12%)	2.76 (0.24%)	0.40 (0.03%)	38.38 (−3%)	21.70 (2%)
	Mixed gardens	98.88 (−6%)	205.20 (12%)	977.72 (56%)	31.18 (1.8%)	6.67 (0.38%)	198.81 (−11%)	218.45 (13%)
	Bare land	0.05 (−29%)	0	0	0.03 (17%)	0	0.09 (−52%)	0
	Built-up	64.95 (−19%)	0.89 (0.26%)	4.12 (−1%)	25.21 (7%)	196.09 (57%)	46.86 (−14%)	3.98 (−1%)
	Paddy fields	162.38 (14%)	51.90 (5%)	122.26 (11%)	42.58 (4%)	17.88 (2%)	641.11 (−57%)	92.82 (8%)
	Shrubs	5.54 (−10%)	2.11 (−4%)	25.30 (44%)	1.15 (2%)	0.29 (−1%)	5.55 (−10%)	17.65 (31%)

in 2013. According to Thonfeld *et al.* (2020), the change in forest cover may have minor impacts on biodiversity and ecosystem services compared to the stronger effects from the conversion of natural or non-agricultural landscapes such as forests, shrubs, and mixed gardens to agricultural and nonvegetated land uses (e.g., drylands, paddy fields, built-up areas, and bare lands).

Vegetation index in the study area

The NDVI map in this study ranged from 0.0796807 to 0.880033 (Fig. 3). Higher NDVI values were distributed in the northwest compared to other parts of the Rancakalong District because there was an undisturbed forest in this area. The high NDVI value was indicative that the green biomass was mainly distributed in the northwest area (Bosino *et al.,* 2019). Conversely, the lowest NDVI was distributed in the south, which contained the majority of built-up areas and bare lands. This situation was mainly attributed

to the land-clearing process for the construction of the Cisumdawu Highway, which passes through Rancakalong District. According to Suharyanto *et al.* (2021), man-made materials can strongly reflect solar radiation, resulting in a massive reduction in NDVI. High NDVI values, which indicate the presence of dense vegetation, were evident in forest areas and some mixed garden areas. Although some areas were considered bare lands, the absence of a negative value indicates there were still vegetated parts of these areas. This evidence of vegetation might be related to replanting activities and succession progress in abandoned areas following land clearing. In turn, NDVI can provide insight and predict vegetation recovery after some disturbance events (Saito *et al.,* 2022). Moderate vegetation cover (indicated in yellow) was largely located in some nonperennial plant-based agricultural lands, such as paddy fields and drylands. The NDVI value distribution in the study site can superficially predict the amount of
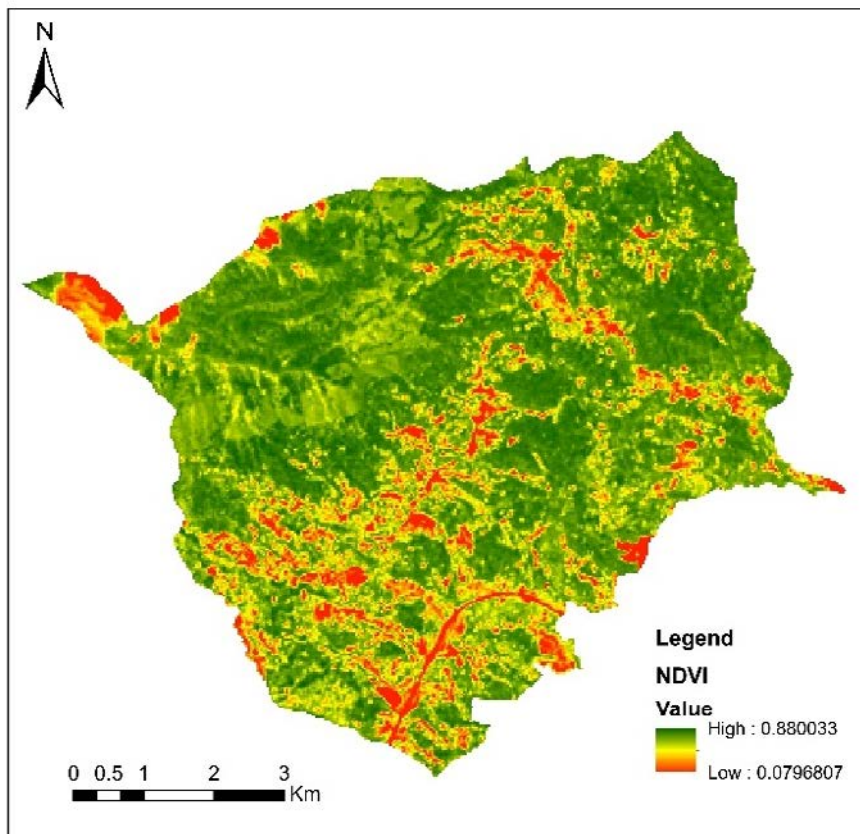
Fig. 3: Map of NDVI distribution in Rancakalong District
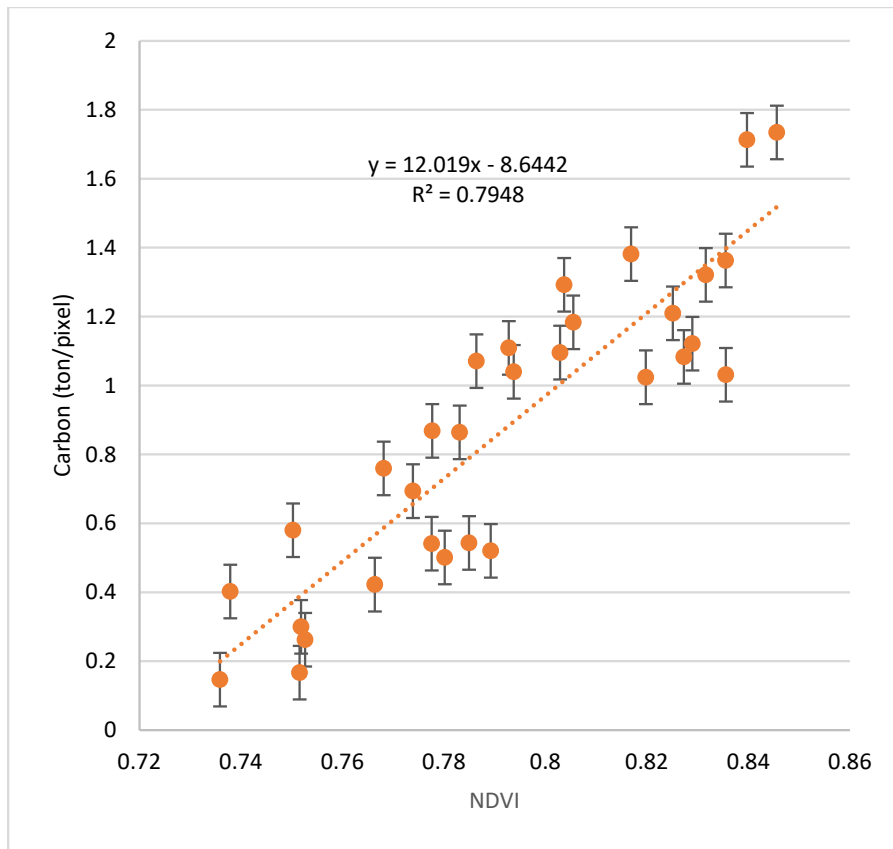
Fig. 4: Scatterplot of NDVI and aboveground carbon stocks in a linear regression model

vegetation biomass (Astsatryan *et al.,* 2015), which was useful in extrapolating the aboveground biomass and carbon content to a landscape scale.

Extrapolation of field carbon inventory data to the landscape scale

The aboveground carbon stock estimation model was built using correlation analysis. A simple linear regression analysis was carried out to identify the degree of correlation between NDVI values and the plot-level result of carbon stocks. As shown in Fig. 4, the regression model revealed a positive relationship between aboveground carbon stocks in the field and NDVI values. The scatterplot shows a positive trend: the higher the NDVI value, the higher the aboveground carbon stocks in the study site. A determination value (R^2) of 0.7948 shows a significant correlation between field measurements of aboveground carbon stocks and NDVI values.

The result shows that approximately 79% of aboveground carbon stocks in the study area can be determined by NDVI values in this regression model, while 21% of aboveground carbon stocks were determined by other factors. This relatively strong determination value suggests that the regression model can effectively extrapolate aboveground carbon stocks to the landscape scale. To demonstrate this, an accuracy test was conducted comparing the aboveground carbon stocks from the model and data from the field measurements in all permanent plots. The SEE test resulted in an estimated error of 0.445195549 tons/pixel. The relatively low estimated error suggests that the simple linear regression is the optimal model for aboveground carbon stock estimation using NDVI as the vegetation index in the study area.

The results of the aboveground carbon stock extrapolation and crop yield data obtained from

Table 3: Carbon pool values (tons/ha/y) for each LULC class in the study site

Code	LULC class name	C-above
1	Drylands	30.90717857
2	Forests	56.93176429
3	Mixed gardens	123.9699638
4	Bare land	0
5	Built-up	0
6	Paddy fields	3.5290878
7	Shrubs	80.03822364
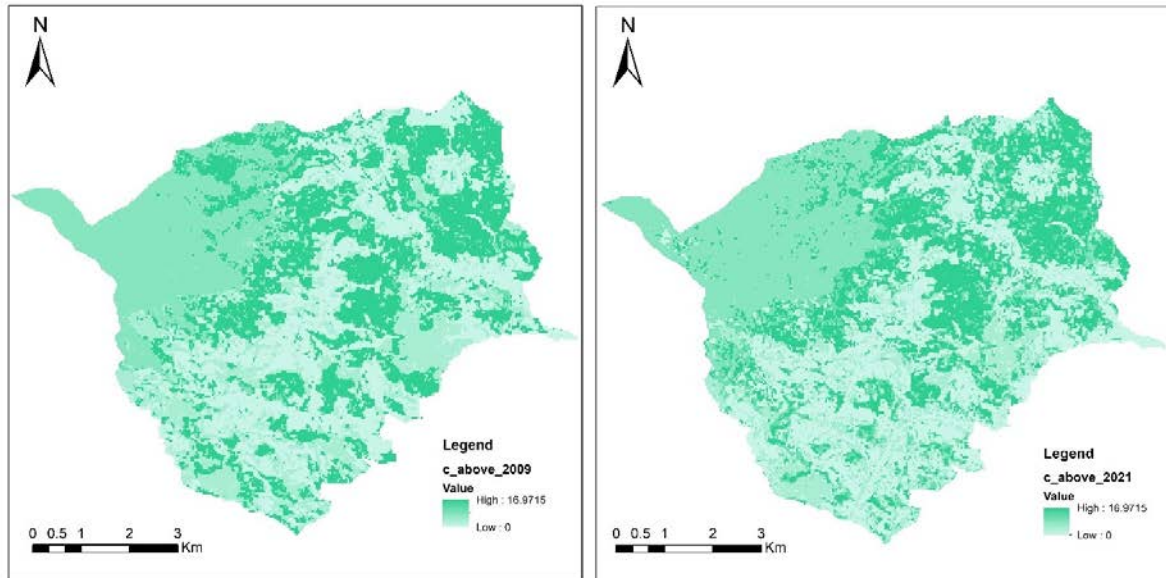
Fig. 5: Distribution of estimated aboveground carbon stocks in 2009 and 2021

GAEZ+ were aggregated and assigned to each LULC class. The aboveground biomass value for built-up and bare land areas was set at zero because an extremely low vegetation cover can be neglected when generating an optimal carbon stock model. This decision followed the assumption that those LULC classes did not have any potential aboveground carbon content. An aboveground carbon pool tabulation for each LULC class is presented in Table 3.

Spatial distribution of carbon stocks

The InVEST carbon storage and sequestration model generated a raster representing the spatial distribution of carbon stocks in the research area (Fig. 5). Between 2009 and 2021, the spatial distribution of aboveground carbon stocks in Rancakalong District became less varied. The highest aboveground carbon stock value in Rancakalong

District was 16.97 tons, which was located in the dense vegetation area. Carbon stock values were generally highest in the western and northeastern regions, where the climate and topographic conditions were favorable for the growth of the forest. These areas were considered part of a mountain range in the study area. Meanwhile, the lowest aboveground carbon stock was 0, as it was assumed that bare land and built-up land did not contain aboveground carbon stock potential in the long term. The lower carbon stock values were mainly distributed in the southern region where drylands and other land uses that had scant carbon stock potential predominated. In particular, the drylands were mainly dominated by upland commodity cultivation with no vegetation stands. As a result, there was less vegetation coverage and relatively low carbon stocks. The spatial distribution of carbon stocks in the study area was related to

the LULC class distribution. The area dominated by dense forest and tree-based agricultural landscapes contained more carbon stocks than the region dominated by undergrowth vegetation-based agriculture and other unused lands, such as the bare lands resulting from land-clearing activities. Between 2009 and 2021, there was a significant decrease in aboveground carbon stocks in the southern areas of Rancakalong District. This reduction is due to widespread conversion of mixed garden locations to built-up and bare land areas. In northeastern areas, the increase in upland agricultural LULC classes resulted in a reduction of vegetation coverage in tree-based agricultural LULC classes. This reduction led to a slight decrease in aboveground carbon stocks in this area. The major causes of vegetation cover reduction were mainly attributed to the conversion of forests and mixed gardens (as the most vegetated LULC classes) to paddy fields. The expansion of paddy fields at the expense of forests and mixed gardens might be driven by population growth coupled with an increase in the requirement for paddy field cultivation as subsistence. Another cause for this vegetation cover reduction might be related to the abandonment of mixed garden areas after harvesting perennials, resulting in the areas being converted to shrublands.

The effect of land use and land cover changes on carbon stocks

The spatial model of aboveground carbon stocks generated by InVEST shows that in 2009, the total stock of aboveground carbon in Rancakalong District was 324,821 tons. In comparison, the total stock of aboveground carbon in 2021 was 313,725 tons. The aboveground carbon stock potential varied among all LULC classes. In 2009, the highest aboveground carbon stocks were from mixed gardens, which had a total carbon stock of 64%. This carbon stock level was followed by forest (20%) and other agricultural LULC classes, namely, drylands (12%) and paddy fields (2%) (Fig. 6). In 2021, the highest aboveground carbon stocks were also in mixed gardens, which contributed 52%. This level was followed by forests (22%), shrubs (15%), and drylands (7%) (Fig. 6). According to the numeric statistics model generated by InVEST, there was a decrease in aboveground carbon density in the study area by 11,096 tons between 2009 and 2021. A significant decrease occurred in the mixed-garden LULC class. The number of aboveground carbon stocks in mixed gardens decreased from 64% to 52%. A decrease in aboveground carbon density also occurred in drylands, with a reduction from 12% to 7%. Conversely, there was an increase in
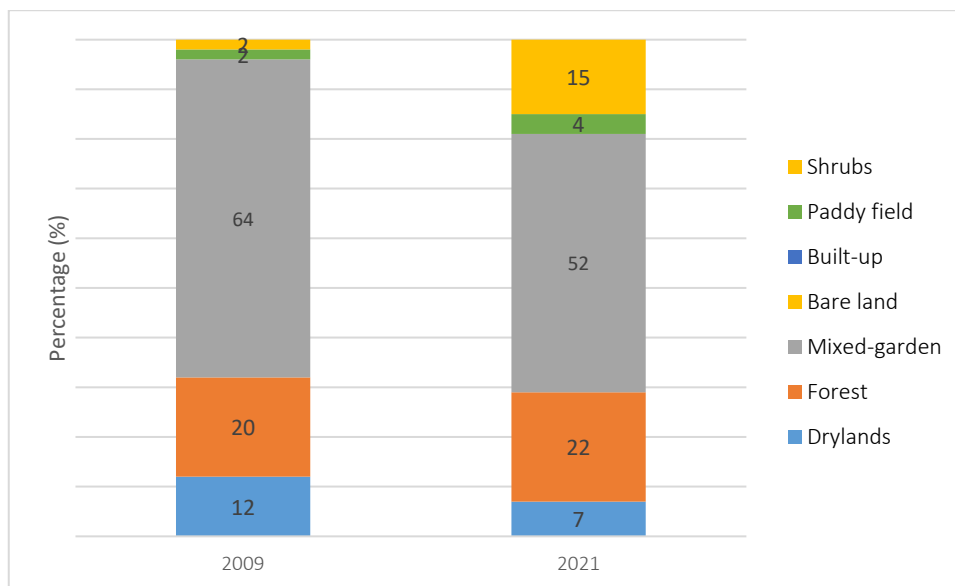
Fig. 6: Percentage of aboveground carbon stock distribution for each LULC class

aboveground carbon stocks in forests (20%–22%), shrubs (2%–15%), and paddy fields (2%–4%) (Fig. 6).

The aboveground carbon stocks of vegetated areas were greater than the potential carbon stocks of other LULC classes. Forests and mixed gardens were considered to be vegetated areas because vegetation stand coverage was dominant in both classes. As shown in Fig. 6, the combined aboveground carbon stocks in forests and mixed gardens were significantly higher than those in other LULC classes (84% in 2009 and 74% in 2021). Forest aboveground carbon density was relatively higher than that in agricultural areas. As presented in Fig. 6, in both 2009 and 2021, forests contributed more carbon storage (20% and 22%, respectively) than agricultural areas, such as drylands (14%) and paddy fields (11%), respectively. However, mixed gardens were the only exception. As agricultural areas, mixed gardens have significantly higher aboveground carbon stock densities than forests. For both 2009 and 2021, mixed gardens contributed more to aboveground carbon stocks than forests, with a comparison of 64% to 20% in 2009 and 52% to 22% in 2021. This advantage is because the total area of the mixed garden was larger than the forest area, as shown in Table 1. In 2009, mixed gardens were the largest LULC class, with an area of 1736.90 ha, compared to forests, which had a total area of 1134.54 ha. Although the forest area increased to 1218.73 ha in 2021, the total area of the mixed gardens was still the largest in the study site, with 1413.36 ha.

Hairiah *et al.* (2011) stated that the aboveground carbon stock potential of forests is relatively higher than that of any other vegetated land cover. However, in this study area, the aboveground carbon stocks in mixed gardens were higher than stocks in forests. This preponderance is associated with the structure and composition of the tree-based farming system. The case study in Rancakalong District, Sumedang, Indonesia shows that different LULC activities lead to variability in aboveground carbon storage potential within all LULC classes in a landscape with a mix of agriculture and forest.

In the study area, more vegetated LULC classes had increased aboveground carbon stock potential compared to less vegetated LULC classes, although less vegetated LULC classes covered a larger area. In comparison to open agricultural areas, shrubs, built-up areas, and bare land, dense forests have higher aboveground carbon stocks. A study conducted by Piyathilake *et al.* (2022) revealed that carbon storage in natural forests was significantly higher than that in agricultural LULC classes, although the area of forest cover was much lower than that in the other LULC classes combined. Additionally, a sparse forest was shown to have more potential for carbon storage than agricultural land (Bera *et al.,* 2022). Carbon storage and sequestration were also positively correlated with the degree of green density of vegetation growth, and a dense forest had the greenest density (Chacko *et al.,* 2018). Confirming these findings, the highest number of aboveground carbon stocks in Rancakalong District was located in the LULC classes with the highest density of vegetation cover. However, in the study site, mixed gardens were the largest contributor to carbon stocks, not forests. Mixed-gardens, which are a tree-based agricultural system, contained the highest number of carbon stocks, even though these stocks were greatly depleted between 2009 and 2021. The percentage of carbon stored in mixed gardens decreased from 64% to 52%, mainly due to a reduction in this LULC class area from 1736.90 ha to 1413.36 ha between 2009 and 2021. However, the carbon density data for mixed gardens may fluctuate concerning the influence of carbon deposition during the harvesting time of vegetation stands. This may result in uncertainty about the change in aboveground carbon stocks over time (Wang *et al.,* 2022). Furthermore, the carbon sequestration and carbon storage potentials of agricultural areas were probably underestimated, as the carbon sinks were potentially offset during harvesting time (Paquit and Mindana, 2017). The fact that mixed gardens had a higher carbon storage potential than forests was related to the structure and composition of the vegetation in this tree-based agricultural system. Mixed gardens, which are generally located on hillslopes of Rancakalong District, are agroforestry systems. They are a common agroforestry system in West Java, Indonesia, and are known locally as *talun* or *kebon tatangkalan* (Parikesit *et al.,* 2005). In the study area, this type of agroforestry comprises bamboo species (*Gigantochloa atter, Schizostachyum brachycladum*, *Dendrocalamus asper*), fruit trees (*Durio zibethinus*, *Artocarpus heterophyllus, Persea americana*), and timber trees

(*Swietenia macrophylla*, *Maesopsis eminii*, and *Tectona grandis*). These trees are cultivated with a mixture of aromatics and rhizomes, such as clover, coffee, ginger, and cardamom. The *talun* gradually evolved from a mixture of annual crops and tree seedlings. The field was frequently abandoned after the annuals were harvested, after which perennials dominated the agricultural area (Christanty *et al.,* 1986). During the abandonment phase, the perennials continually grew and became mature. As the perennials dominated, the agricultural area resembled secondary forest fallow and was essentially a man-made forest (Soemarwoto, 1984). The *talun* consisted of a mixture of perennial trees with a multilayered canopy as a key characteristic of this traditional agroforestry system (Soemarwoto, 1984). The findings on the carbon stock potential of this tree-based *talun* agricultural system corroborated a previous study on aboveground carbon stocks in Rancakalong revealing that the coffee-based agroforestry system had higher carbon storage potential than secondary forests. This greater potential was due to the dominance of sparse vegetation with a smaller diameter in some of the secondary forests (Luth and Setiyono, 2019). The result is in line with findings by Natalia *et al.* (2016), who stated that the basal area of trees is strongly correlated with total carbon stocks in natural forests and agroforestry. This study found that the change in aboveground carbon stocks was mainly attributed to LULC change. There was a decrease in total aboveground carbon stocks by 11,096 tons between 2009 and 2021. This carbon storage reduction was mainly related to urban expansion in Rancakalong District. The construction of the Cisumdawu Highway, which started in 2013, was at the expense of vegetated LULC classes. This construction might have contributed to the reduction in aboveground carbon stocks in the study area. Data from 2021 show that the construction of the highway resulted in a significant increase in bare land cover as a result of LULC conversion from tree-based agroforestry and other agricultural land use classes. A 138.70-ha increase in bare land in 2021 was due to the change in LULC classes with larger carbon inventories, such as mixed gardens, paddy fields, and drylands. This change reduced the total number of aboveground carbon stocks in the Rancakalong District. A study conducted in the Silang-Santa Rosa Watershed in the Philippines also showed that the continuous expansion of urban areas resulted in a decrease in the total number of carbon stocks (Dida *et al.,* 2021). Similarly, the rapid increase in built-up land because of farmland conversion was linked to a decline in carbon storage capability in northwestern China (Liang *et al.,* 2017). The reduction in aboveground carbon stocks was also related to the conversion of forest cover and other vegetated LULC classes into croplands. The findings of Pellikka *et al.* (2018) in Afromontane in Kenya showed that the deterioration of forest cover and shrublands directly caused a reduction in carbon sequestration. In this study, the reduction in aboveground carbon stocks in the vegetated area generally resulted from the abandonment of some mixed gardens after the mature trees were harvested. This process led to the massive conversion of mixed gardens to shrublands between 2009 and 2021, which contain lower aboveground carbon stock potential. As a result, during the fallow period, there were only shrubs and undergrowth vegetation cover. Developing a spatial distribution of aboveground carbon storage within different LULC classes provides information about the potential of different LULC classes in carbon storage and sequestration. The spatial dynamics of aboveground carbon stocks reveal how aboveground carbon stocks fluctuate over time within different LULC classes as a result of anthropogenic interventions such as urban expansion and agricultural management. Carbon stocks in other carbon pools (belowground biomass, soil, litter, and necromass) must be further studied, including the use of higher resolution remote sensing data and enhancing the sample size at the plot level to comprehensively map the dynamics of carbon storage and carbon stock potential in the research area across a variety of land uses. As this study only relies on business-as-usual LULC trends, it is essential to develop various LULC change scenarios. The results of carbon stock estimation and modeling using InVEST should be considered in decision-making processes related to environmental management and regional development plans (spatial plans). These data could be used as a basis for a carbon credit scheme to protect vegetated areas and combat climate change.

Tree-based agricultural systems (mixed gardens) have shown significant potential in carbon storage.

Therefore, this LULC class needs appropriate management strategies to enhance carbon storage potential while simultaneously reducing carbon emissions. Conservative farming practices in the form of mixed gardens should be enhanced to boost subsistence farming without undermining the potential of this agricultural landscape to contribute to carbon sequestration and climate change mitigation.

CONCLUSION

This study emphasizes the correlation between LULC changes and aboveground carbon stocks. Furthermore, this work examines how LULC conversions such as urban expansion and agricultural management put direct pressure on carbon storage potential in different LULC classes. Massive construction and agricultural expansion are still occurring in the study area; therefore, it is critical to detect the carbon stock levels affected by LULC changes. The present study attempts to incorporate a few ground-based inventories of carbon stocks into GIS and remote sensing approaches and integrates the inventory data with the InVEST spatial carbon dynamics model. The results of supervised classification on remotely sensed satellite images showed that vegetated land was predominant in 2009 and 2021. Vegetation covered 51% of the total area in 2009 and increased by 6% in 2021, resulting in 57% of vegetation area coverage. Regarding agricultural area, mixed gardens and drylands decreased between 2009 and 2021 by 6% and 8%, respectively. Meanwhile, paddy fields were the only agricultural land use to increase by 2% between 2009 and 2021. The bare land and built-up expansion related to the observed land clearing for the Cisumdawu Highway mainly came from the conversion of mixed gardens, paddy fields, and drylands. This study has demonstrated that LULC changes in the Rancakalong District have caused a reduction in aboveground carbon stocks by 11,096 tons between 2009 and 2021. Based on the results of the InVEST spatial and statistical models, a reduction in aboveground carbon stocks occurred in the mixed gardens and drylands, with the highest reduction occurring in mixed gardens. Indeed, the number of aboveground carbon stocks in mixed gardens declined from 64% to 52%. In those mixed gardens were the most common LULC

class in the study area in both 2009 and 2021, the massive reduction in this agricultural area caused a significant decrease in aboveground carbon stocks, although a slight increase in aboveground carbon stocks occurred in forests, shrubs, and paddy fields. This shortage of carbon stock potential was mainly attributed to the abandonment of this tree-based agricultural system after harvesting and led to the massive conversion of mixed gardens to shrublands, which contain lower aboveground carbon stock potential. The construction of the Cisumdawu Highway, which started in 2013, was at the expense of vegetated LULC classes. This development might have contributed to the reduction in aboveground carbon stocks in the study area. The results of remotely sensed data from 2021 show that the construction of the highway resulted in a significant increase in bare land cover as a result of LULC conversion from tree-based agroforestry and other agricultural land use classes. A 138.70-ha increase in bare land in 2021 was due to the conversion of LULC classes to those with larger carbon stocks, particularly mixed gardens. In the future, it is crucial to conserve this bioproduction system with long-term protection mechanisms as this tree-based agricultural system (mixed gardens) showed great potential in aboveground carbon storage. The model should be considered in decision-making processes related to environmental management and regional development plans (spatial plans). Further studies may consider alternative scenarios in LULC changes.

AUTHOR CONTRIBUTIONS

ACKNOWLEDGEMENT

CONFLICT OF INTEREST

OPEN ACCESS

PUBLISHER'S NOTE

GJESM Publisher remains neutral with regard to jurisdictional claims in published maps and institutional afflictions.

ABBREVIATIONS

%	Percent
θ_s	Angle of the sun's zenith in degrees
ρ	Wood density
$\rho\lambda'$	Top of atmosphere reflectance
ρ_p	Planetary reflectance
ρ_λ	Surface reflectance
π	Phi
%	Percent
A_L	The metadata's additive rescaling factor
$\bar{A}_\rho$	Additive rescaling factor from the metadata for each band
AGB	Total aboveground biomass
ArcMap	Geographic information as a collection of layers and other elements in a map
C	Celsius
CO_2	Carbondioxide
csv	Comma separated value
d	The astronomic distance between earth and sun
DBH	Diameter at breast height
DN	Digital numbers
DOS1	Dark object subtraction 1
E_{down}	The downwelling diffuse irradiance
$ESUN_\lambda$	The mean value of solar exo-atmospheric irradiances
GIS	Geographic information systems
gr/cm^3	Gram per cubic centimeter
GAEZ+	Global agro-ecological zones' +
Gt	Gigatons
ha	Hectares
InVEST	Integrated valuation of ecosystem services and tradeoffs
IPCC	Intergovernmental Panel on Climate Change
km	Kilometers
L_λ	Top of atmosphere spectral radiance
L_p	Path radiance
LULC	Land use and land cover
M_ρ	Metadata-derived band-specific multiplicative rescaling factor

M_L	Metadata-derived multiplicative rescaling factor
m	Meters
m²	Square meters
mm/y	Milimeters per year
MLC	Maximum likelihood classification
MTL	Metadata text file extension
MW	Megawatts
n	Number of plots
NDVI	Normalized difference vegetation index
NIR	Near-infrared band
OLI	Operational land imager
ppm	Parts per million
Q_{cal}	Standard product pixel values or digital number value of a specific pixel
SCP	Semiautomatic classification plugin
SEE	Standard errors of estimate
T	Tree height
T_v	Atmospheric transmittance in the viewing direction
T_z	Atmospheric transmittance in the illumination direction
tiff	Temporary instruction file format
TM	Thematic mapper
TOA	Top of atmosphere
tons/ha	Tons per hectare
y_i	Carbon value in plot number-i

REFERENCES

Arredondo-Trapero, F.G.; Guerra-Leal, E.M.; Kim, J., (2023). Effectiveness of the voluntary disclosure of corporate information and its commitment to climate change. Global J. Environ. Sci. Manage., 9(4): 1033-1048 **(16 pages)**.

Astsatryan, H.; Hayrapetyan, A.; Narsisian, W.; Asmaryan, S.; Saghatelyan, A.; Muradyan, V.; Giuliani, G.; Guigoz, Y.; Ray, N., (2015). An interoperable cloud-based scientific GATEWAY for NDVI time series analysis. Comput. Stand. Interfaces. 4: 79-84 **(6 pages).**

Bagstad, K.J.; Semmens, D.J.; Waage, S.; Winthrop, R., (2013). A comparative assessment of decision-support tools for ecosystem services quantification and valuation. Ecosyst. Serv., 5: 27-39 **(13 pages).**

Basalumi, L.; Kilawe, C.J.; Mauya, E.W., (2018). Linking ground forest inventory and NDVI in mapping above ground carbon stock in Kasane Forest Reserve, Botswana. Open J. For., 8(3): 429-438 **(10 pages).**

Batsaikhan, B.; Lkhamjav, O.; Batsaikhan, G.; Batsaikhan, N.; Norovsuren, B., (2020). Carbon stock estimation using remote sensing data and field measurement in haloxylon ammodendron dominant winter cold desert region of Mongolia. In XXIV ISPRS Congress, Commission III (Volume V-3-2020)- 2020 edition.

Bera, B.; Bhattacharjee, S.; Sengupta, N.; Shit, P.K.; Adhikary, P.P.; Sengupta, D.; Saha, S., (2022). Significant reduction of carbon stocks and changes of ecosystem service valuation of Indian Sundarban. Sci. Rep., 12: 7809 **(17 pages).**

Bosino, A.; Omran, A.; Maerker, M., (2019). Identification, characterisation and analysis of the Oltrepo Pavese calanchi in the Northern Apennines (Italy). Geomorphology, 340: 53-66 **(14 pages)**.

Cahyono, W.; Parikesit; Joy, B.; Setyawati, W.; Mahdi, R., (2022). Projection of CO_2 emissions in Indonesia. In 2nd International Conference on Chemical Engineering and Applied Sciences. Semarang, Indonesia 3 - 4 November. UNDIP: Indonesia.

Calderón-Contreras, R.; Quiroz-Rosas, L.E., (2017). Analysing scale, quality and diversity of green infrastructure and the provision of urban ecosystem services: A case from Mexico City. Ecosyst. Serv., 23: 127-137 **(11 pages)**.

Chacko, S.; Ravichandran, C.; Vairavel, S.M.; Mathew, J., (2018). Employing measurers of spatial distribution of carbon storage in Periyar Tiger Reserve, Southern Western Ghats, India. J. Geovisualization Spatial Anal., 3(1): 1-7 **(7 pages)**.

Chander, G.; Markham, B., (2003). Revised Landsat-5 TM radiometric calibration procedures and postcalibration dynamic ranges. IEEE Trans. Geosci. Remote Sens., 41(11): 2674–2677 **(4 pages)**.

Chave, J.; Andalo, C.; Brown, S.; Cairns, M. A.; Chambers, J.Q.; Eamus, D.; Fölster, H.; Fromard, F.; Higuchi, N.; Kira, T.; Lescure, J.-P.; Nelson, B.W.; Ogawa, H.; Puig, H.; Riéra, B.; Yamakura, T., (2005). Tree allometry and improved estimation of carbon stocks and balance in tropical forests. Oecologia. 145(1): 87-99 **(13 pages)**.

Chavez Jr., P.S., (1989). Radiometric calibration of Landsat Thematic Mapper multispectral images. Photogramm. Eng. Remote Sens., 55(9): 1285-1294 **(10 pages)**.

Christanty, L.; Abdoellah, O.S.; Marten, G.; Iskandar, J., (1986). Traditional agriculture in southeast Asia: A human ecology perspective. Westview Press.

Cong, W.; Sun, X.; Guo, H.; Shan, R., (2020). Comparison of the SWAT and InVEST models to determine hydrological ecosystem service spatial patterns, priorities and trade-offs in a complex basin. Ecol. Indic., 112: 1-13 **(13 pages)**.

Coutinho, H.L.C.; Noellemeyer, E.; Balieiro, F.de C.; Piñeiro,

G.; Fidalgo, E.C.C.; Martius, C.; Silva, C. F.da., (2015). Impacts of land-use change on carbon stocks and dynamics in central-southern South American biomes: Cerrado, Atlantic Forest and Southern Grasslands, in : Banwart S.A., Noellemeyer E., Milne, E. (Eds.), Soil carbon: science, management and policy for multiple benefits. CABI Digital Library.

Darmawan, A.A.; Ariyanto, D.P.; Basuki, T.M.; Syamsiyah, J.; Dewi, W.S., (2022). Biomass accumulation and carbon sequestration potential in varying tree species, ages and densities in Gunung Bromo Education Forest, Central Java, Indonesia. Biodiversitas. 23(10): 5093-5100 **(8 pages)**.

Davies, T.; Everard, M.; Horswell, M., (2016). Community-based groundwater and ecosystem restoration in semi-arid north Rajasthan (3): evidence from remote sensing. Ecosyst. Serv., 21(2016): 20-30 **(11 pages)**.

Dewanto, B.E.B.; Jatmiko, R.H., (2021). Estimation of aboveground carbon stock using SAR Sentinel-1 imagery in samarinda city. IJReSES. 18(1): 103-116 **(14 pages)**.

Dida, J.J.; Tiburan Jr.,C.; Tsutsumida, N.; Saizen, I., (2021). Carbon stock estimation of selected watersheds in Laguna, Philippines Using InVEST. Philipp J. Sci., 150(2): 501-513 **(13 pages)**.

FAO, (2016). Global forest resources assessment 2015: How are the world's forests changing? (second edition). Food and Agriculture Organization of the United Nations, Rome.

Forestry Economics and Policy Division, (2010). Global forest resources assessment 2010—main report. Food and Agriculture Organization of the United Nations, Rome.

Frolking, S.; Wisser, D.; Grogan, D.; Proussevitch, A.; Glidden, S., (2020). GAEZ+_2015 crop yield. Harvard Dataverse.

Frimawaty, E.; Ilmika, A.; Sakina, N.A; Mustabi. J., (2023). Climate change mitigation and adaptation through livestock waste management. Global J. Environ. Sci. Manage., 9(4): 691-706 (16 pages).

Hairiah, K.; Dewi, S.; Agus, F.; Velarde, S.; Ekadinata, A.; Rahayu, S.; van Noordwijk, M., (2011). Measuring carbon stocks across land use systems: a manual. World Agroforestry Centre (ICRAF) SEA Region Office, Bogor.

Harper, A.B.; Wiltshire, A.J.; Cox, P.M.; Friedlingstein, P.; Jones, C.D.; Mercado, L.M.; Sitch, S.; Williams, K.; Duran-Rojas, C., (2018). Vegetation distribution and terrestrial carbon cycle in a carbon cycle configuration of JULES4.6 with new plant functional types. Geosci. Model Dev., 11(7): 2857-2873 **(17 pages)**.

Hassan, W.H.; Nile, B.K., (2021). Climate change and predicting future temperature in Iraq using CanESM2 and HadCM3 modeling. Model. Earth Syst. Environ., 7(2): 737-748 **(12 pages)**.

Hua, A.K.; Ping, O.W., (2018). The influence of land-use/land-cover changes on land surface temperature: A case study of Kuala Lumpur metropolitan city. Eur. J. Remote Sens., 51(1): 1049-1069 **(21 pages)**.

IPCC, (2022). Global Warming of 1.5°C: IPCC special report on impacts of global warming of 1.5°c above pre-industrial levels in context of strengthening response to climate change, sustainable development, and efforts to eradicate poverty (1st ed.). Cambridge University Press, Cambridge.

IPCC, (2014). AR5 synthesis report: climate change 2014: Intergovernmental Panel for Climate Change.

Jagdish, J.; Erayya; Makanur, B.; Sajeesh, P.K.; Managanvi, K., (2013). Prospects for mitigation of greenhouse gas emission: in context to agriculture and climate change. Environ. Ecol., 31(2): 551-557 **(7 pages)**.

Jamali, S.; Seaquist, J.W.; Ardö, J.; Eklundh, L., (2011). Investigating temporal relationships between rainfall, soil moisture and Modis-Derived NDVI and EVI for six sites in Africa. in 34th International Symposium on Remote Sensing of Environment. Sydney, Australia 10-15 April. International Center for Remote Sensing of Environment: Tucson.

Javaherian, M.; Ebrahimi, H.; Aminnejad, B., (2021). Prediction of changes in climatic parameters using CanESM2 model based on RCP scenarios (case study): Lar dam basin. Ain. Shams. Eng. J., 12(1): 445-454 **(10 pages)**.

Jaya, L.M.G.; Saputra, R.A.; Idrus, S.H., (2022). Using support vector machine to identify land cover change during covid-19 pandemic in Komodo National Park, Indonesia. Geogr. Environ. Sustainability. 15(3): 70-79 **(10 pages)**.

Jiang, H.; Wu, W.; Wang, J.; Yang, W.; Gao, Y.; Duan, Y.; Ma, G.; Wu, C.; Shao, J., (2021). Mapping global value of terrestrial ecosystem services by countries. Ecosyst. Serv., 52(2021): 101361 **(10 pages)**.

Karbassi, A.R.; Tajziehchi, S.; Afshar, S., (2015). An investigation on heavy metals in soils around oil field area. Global J. Environ. Sci. Manage., 1(4): 275-282 **(8 pages).**

Khaerani, R.; Sitorus, S.R.P.; Rusdiana, O., (2018). Analysis of land use deviation based on spatial plan in Sumedang Regency. TATALOKA. 20(4): 399-409 **(11 pages)**.

KLHK, (2018). The state of Indonesia's forests 2018. Ministry of Environment and Forestry Republic of Indonesia (KLHK), Jakarta.

Kusumaningtyas, M.A.; Kepel, T.L.; Solihuddin, T.; Lubis, A.A.; Putra, A.D.P.; Sugiharto, U.; Ati, R.N.A.; Salim, H.L.; Mustikasari, E.; Heriati, A.; Daulat, A.; Sudirman, N.; Suryono, D.D.; Rustam, A., (2022). Carbon sequestration potential in the rehabilitated mangroves in Indonesia. Ecol. Res., 37(1): 80-91 **(12 pages)**.

Lahiji, R. N.; Dinan, N.M.; Liaghati, H.; Ghaffarzadeh, H.; Vafaeinejad, A., (2020). Scenario-based estimation of catchment carbon storage: Linking multi-objective land allocation with InVEST model in a mixed agriculture-forest landscape. Front. Earth Sci., 14(3): 637-646 **(10 pages)**.

Latifah, S.; Muhdi, M.; Purwoko, A.; Tanjung, E., (2018). Estimation of aboveground tree biomass Toona sureni and Coffea arabica in agroforestry system of Simalungun, North Sumatra, Indonesia. Biodiversitas. 19(2): 670-675 **(6 pages)**.

Lee, H.; Seo, B.; Cord, A.F.; Volk, M.; Lautenbach, S., (2022). Using crowdsourced images to study selected cultural ecosystem services and their relationships with species richness and carbon sequestration. Ecosyst. Serv., 54(2022): 101411 **(12 pages)**.

Li, S.; Wang, W.; Ganguly, S.; Nemani, R.R., (2018). Radiometric characteristics of the Landsat collection 1 dataset. Int. J. Adv. Remote Sens., 7(3): 203-217 **(14 pages)**.

Liang, Y.; Liu, L.; Huang, J., (2017). Integrating the SD-CLUE-S and InVEST models into assessment of oasis carbon storage in northwestern China. PLoS One. 12(2): e0172494 **(15 pages)**.

Liu, J.; Sleeter, B.M.; Zhu, Z.; Heath, L.S.; Tan, Z.; Wilson, T.S.; Sherba, J.; Zhou, D., (2016). Estimating carbon sequestration in the piedmont ecoregion of the United States from 1971 to 2010. Carbon Balance Manage., 11(10): 10-22 **(13 pages)**.

Liu, J.; Mason, P.J.; Bryant, E.C., (2018). Regional assessment of geohazard recovery eight years after the Mw7.9 Wenchuan earthquake: A remote-sensing investigation of the Beichuan region. Int. J. Remote Sens., 39(6): 1671-1695 **(25 pages)**.

Luth, F.; Setiyono, H., (2019). Capacity of coffee-based agroforestry in carbon storage. Paspalum, 7(1): 34-41 **(8 pages)**.

Marchetti, Z.Y.; Minotti, P.G.; Ramonell, C.G.; Schivo, F.; Kandus, P., (2016). NDVI patterns as indicator of morphodynamic activity in the middle Paraná River floodplain. Geomorphology, 253: 146-158 **(13 pages)**.

Massetti, A.; Gil, A., (2020). Mapping and assessing land cover/land use and aboveground carbon stocks rapid changes in small oceanic islands' terrestrial ecosystems: a case study of Madeira Island, Portugal (2009–2011). Remote Sens. Environ., 239(2020): 111625 **(11 pages)**.

Masripatin, N.; Gustan, P.; Wayan, S.; Chairil, A.; Ari, W.; Dyah, S.; Arief; Niken, S.; Mega, L.; In-dartik; Wening, W.; Saptadi, D.; Ika, H.; Heriyanto, N.; Haris, S.; Ratih, D.; Dian, A.; Haruni, K.; Bayu, S., (2010). Carbon stocks in many types of forests and plants in indonesia. Pusat Penelitian dan Pengembangan Perubahan Iklim dan Kebijakan, Bogor.

Millennium Ecosystem Assessment, (2005). Ecosystems and human well-being: wetlands and water synthesis: a report of the Millennium Ecosystem Assessment. World Resources Institute, Washington DC.

Moran, M.S.; Jackson, R.D.; Slater, P.N.; Teillet, P.M., (1992). Evaluation of simplified procedures for retrieval of land surface reflectance factors from satellite sensor output. Remote Sens. Environ., 41(2): 169-184 **(16 pages)**.

Natalia, D.; Arisoesilaningsih, E.; Hairiah, K., (2016). Are high carbon stocks in agroforests and forest associated with high plant species diversity? AGRIVITA. 39(1): 74-82 **(9 pages)**.

Nelson, E.; Mendoza, G.; Regetz, J.; Polasky, S.; Tallis, H.; Cameron, Dr.; Chan, K.M.; Daily, G.C.; Goldstein, J.; Kareiva, P.M.; Lonsdorf, E.; Naidoo, R.; Ricketts, T.H.; Shaw, Mr., (2009). Modeling multiple ecosystem services, biodiversity conservation, commodity production, and tradeoffs at landscape scales. Front. Ecol. Environ., 7(1): 4-11 **(8 pages)**.

Nijhawan, R.; Jain, K., (2018). Glacier terminus position monitoring and modeling using remote sensing data, in: M. Singh, P.K., Gupta, V., Tyagi, J., Flusser, Ören, T. (Eds.), Advances in computing and data sciences. Springer Singapore. Singapore.

Ostadhashemi, R.; Rostami, S.T.; Roehle, H.; Mohammadi, L.S., (2014). Estimation of biomass and carbon storage of tree plantations in northern Iran. J. For. Sci., 60(9): 363-371 **(9 pages)**.

Paquit, J.; Mindana, F., (2017). Modeling the spatial pattern of carbon stock in Central Mindanao University using InVEST tool. J. Bio. Environ. Sci., 10(4): 103-113 **(11 pages).**

Parikesit; Takeuchi, K.; Tsunekawa, A.; Abdoellah, O.S., (2005). Kebon tatangkalan: a disappearing agroforest in the Upper Citarum Watershed, West Java, Indonesia. Agrofor. Syst., 63(2): 171-182 **(12 pages)**.

Pellikka, P.K.E.; Heikinheimo, V.; Hietanen, J.; Schäfer, E.; Siljander, M.; Heiskanen, J., (2018). Impact of land cover change on aboveground carbon stocks in Afromontane landscape in Kenya. Appl. Geogr., 94: 178-189 **(12 pages)**.

Piyathilake, I.D.U.H.; Udayakumara, E.P.N.; Ranaweera, L.V.; Gunatilake, S.K., (2022). Modeling predictive assessment of carbon storage using InVEST model in Uva province, Sri Lanka. Model. Earth Syst. Environ., 8(2): 2213-2223 **(11 pages)**.

Posner, S.; Verutes, G.; Koh, I.; Denu, D.; Ricketts, T., (2016). Global use of ecosystem service models. Ecosyst. Serv, 17(2016): 131-141 **(11 pages)**.

Rouse, J.W.Jr.; Haas, R.H.; Schell, J.A.; Deering, D.W., (1974). Monitoring vegetation systems in the great plains with erts. NASA Special Publication, Washington DC.

Saito, H.; Uchiyama, S.; Teshirogi, K., (2022). Rapid vegetation recovery at landslide scars detected by multitemporal high-resolution satellite imagery at ASO volcano, Japan. Geomorphology. 398(2022): 107989 **(9 pages)**.

Sampurno, R.M.; Thoriq, A., (2016). Land cover classification using Landsat 8 Operational Land Imager (OLI) data in Sumedang Regency. Teknotan. 10(2): 61-70 **(10 pages)**.

Senseman, G.M.; Bagley, C.F.; Tweddale, S.A., (1995). Accuracy assessment of the discrete classification of remotely-sensed digital data for landcover mapping. US Army Corps of Engineers, Virginia.

Sharp, R.; Douglass, C.; Wolny, S.; Arkema, K.; Bernhardt, J.; Bierbower, N.; Chaumont, N.; Denu, D.; Fisher, D.; Glowinski, K.; Griffin, R.; Guannel, G.; Guerry, A.; Johnson, J.; Hamel, P.; Kennedy, C.; Kim, C.K.; Lacayo, M.; Lonsdorf, E.; Mandle, L.; Rogers, L.; Silver, J.; Toft, J.; Verutes, G.; Vogl, A.L.; Wood, S.; Wyatt, K., (2018). InVEST 3.7.0 user's guide. The Natural Capital Project, Stanford University,

University of Minnesota, The Nature Conservancy, and World Wildlife Fund, California.

Sharp, R.; Douglass, C.; Wolny, S.; Arkema, K.; Bernhardt, J.; Bierbower, N.; Chaumont, N.; Denu, D.; Fisher, D.; Glowinski, K.; Griffin, R.; Guannel, G.; Guerry, A.; Johnson, J.; Hamel, P.; Kennedy, C.; Kim, C.K.; Lacayo, M.; Lonsdorf, E.; Mandle, L.; Rogers, L.; Silver, J.; Toft, J.; Verutes, G.; Vogl, A.L.; Wood, S.; Wyatt, K., (2020). InVEST 3.10.2 user's guide. The Natural Capital Project, Stanford University, University of Minnesota, The Nature Conservancy, and World Wildlife Fund, California.

Shrestha, M.; Piman, T.; Grünbühel, C., (2021). Prioritizing key biodiversity areas for conservation based on threats and ecosystem services using participatory and GIS-based modeling in Chindwin River Basin, Myanmar. Ecosyst. Serv., 48: 101244 **(11 pages)**.

Situmorang, J.P.; Sugianto, S.; Darusman., (2016). Estimation of carbon stock stands using EVI and NDVI vegetation index in production forest of Lembah Seulawah Sub-district, Aceh Indonesia. Aceh Int. J. Sci. Technol., 5(3): 126-139 **(14 pages)**.

Smith, G., (2015). Essential statistics, regression, and econometrics. Academic Press, California.

Soemarwoto, O., (1984). The talun-kebun system, a modified shifting cultivation, in West Java. The Environmentalist. 4(1984): 96-98 **(3 pages)**.

Solomon, N.; Birhane, E.; Tadesse, T.; Treydte, A.C.; Meles, K., (2017). Carbon stocks and sequestration potential of dry forests under community management in Tigray, Ethiopia. Ecol. Processes. 6(1): 20-30 **(11 pages)**.

Solomon, N.; Pabi, O.; Annang, T.; Asante, I.K.; Birhane, E., (2018). The effects of land cover change on carbon stock dynamics in a dry Afromontane forest in northern Ethiopia. Carbon Balance Manage., 13(1): 14-26 **(13 pages)**.

Suharyanto, A.; Maulana, A.; Suprayogo, D.; Devia, Y.P.; Kurniawan, S., (2023). Land surface temperature changes caused by land cover/ land use properties and their impact on rainfall characteristics. Global J. Environ., Sci. Manage., 9(3): 353-372 **(20 pages)**.

Sumedang Regency, (2019). Decree of Sumedang Regent No. 51 Year 2019 : strategic plan for Rancakalong District, 2018—2023.

Tang, Y.; Quaqin, S.; Tiezhu, S.; Zhensheng, L.; Guofeng, W., (2022). Spatiotemporal dynamics of forest ecosystem carbon budget in Guizhou: customisation and application of the CBM-CFS3 model for China. Carbon Balance Manage., 17(1): 10-33 **(23 pages)**.

Thom, D.; Rammer, W.; Seidl, R., (2017). The impact of future forest dynamics on climate: Interactive effects of changing vegetation and disturbance regimes. Ecol. Monogr., 87(4): 665-684 **(19 pages)**.

Thonfeld, F.; Steinbach, S.; Muro, J.; Hentze, K.; Games, I.; Näschen, K.; Kauzeni, P.F., (2020). The impact of anthropogenic land use change on the protected areas of the Kilombero catchment, Tanzania. IISPRS J. Photogramm. Remote Sens., 168: 41-55 **(15 pages)**.

Toru, T.; Kibret, K., (2019). Carbon stock under major land use/land cover types of Hades sub-watershed, astern Ethiopia. Carbon Balance Manage., 14(1): 7-20 **(14 pages)**.

Vafaei, S.; Soosani, J.; Adeli, K.; Fadaei, H.; Naghavi, H.; Pham, T.D.; Tien B.D., (2018). Improving accuracy estimation of forest aboveground biomass based on incorporation of ALOS-2 PALSAR-2 and Sentinel-2a imagery and machine learning: a case study of the hyrcanian forest area (Iran). Remote Sens., 10(2): 172-192 **(21 pages)**.

Wang, L.; Zhu, R.; Yin, Z.; Chen, Z.; Fang, C.; Lu, R.; Zhou, J.; Feng, Y., (2022). Impacts of land-use change on the spatio-temporal patterns of terrestrial ecosystem carbon storage in the Gansu Province, Northwest China. Remote Sens., 14(13): 3164-3190 **(27 pages)**.

Wani, A.A.; Bhat, A.F.; Gatoo, A.A.; Zahoor, S.; Mehraj, B.; Najam, N.; Wani, Q.S.; Islam, M.A.; Murtaza, S.; Dervash, M.A.; Joshi, P.K., (2021). Assessing relationship of forest biophysical factors with NDVI for carbon management in key coniferous strata of temperate Himalayas. Mitigation Adapt. Strategies Global Change. 26(1): 1-22 **(23 pages)**.

Yesserie, A., (2009). Spatio-temporal land use/land cover changes analysis and monitoring in the Valencia Municipality, Spain. Ph.D. Dissertation, Universitat Jaume I Castellón, Spain.

Zanne, A.E.; Lopez-Gonzalez, G.; Coomes, D.A.; Ilic, J.; Jansen, S.; Lewis, S.L.; Miller, R.B.; Swenson, N.G.; Wiemann, M.C.; Chave, J., (2009). Towards a worldwide wood economics spectrum (Version 5, p. 2047488 bytes). Dryad.

Zhang, C.; Chen, K.; Liu, Y.; Kovacs, J.M.; Flores-Verdugo, F.; Santiago, F.J.F.de., (2012). Spectral response to varying levels of leaf pigments collected from a degraded mangrove forest. J. Appl. Remote Sens., 6(1): 063501 **(14 pages)**.

Zhao, K.; Wulder, M.A.; Hu, T.; Bright, R.; Wu, Q.; Qin, H.; Li, Y.; Toman, E.; Mallick, B.; Zhang, X.; Brown, M., (2019). Detecting change-point, trend, and seasonality in satellite time series data to track abrupt changes and nonlinear dynamics: a bayesian ensemble algorithm. Remote Sens. Environ., 232(2019): 111181 **(20 pages)**.

Zhao, Z.; Liu, G.; Mou, N.; Xie, Y.; Xu, Z.; Li, Y., (2018). Assessment of carbon storage and its influencing factors in Qinghai-Tibet Plateau. Sustainability. 10(6): 1864-1880 **(17 pages)**.

Zhu, X.; Liu, D., (2015). Improving forest aboveground biomass estimation using seasonal Landsat NDVI time-series. ISPRS J. Photogramm. Remote Sens., 102: 222-231 **(10 pages)**.

AUTHOR (S) BIOSKETCHES

Malik, A.D., M.Sc., Assistant Professor, Center for Environment and Sustainability Science, Universitas Padjadjaran, Bandung, West Java, Indonesia.
- Email: *annas12001@mail.unpad.ac.id*
- ORCID: 0000-0003-0588-387X
- Web of Science ResearcherID: HZL-2698-2023
- Scopus Author ID: 57683705500
- Homepage: https://cess.unpad.ac.id/easia_annas/

Arief, M.C.W., Ph.D., Associate Professor, Department of Fisheries, Faculty of Fisheries and Marine Science, Universitas Padjadjaran, Sumedang, West Java, Indonesia.
- Email: *mochamad.candra@unpad.ac.id*
- ORCID: 0000-0003-3077-5934
- Web of Science ResearcherID: HZL-4715-2023
- Scopus Author ID: 56469720200
- Homepage: https://fpik.unpad.ac.id/en/program-studi-perikanan/

Withaningsih, S., Ph.D., Associate Professor, Sustainability Science Masters Study Program, Graduate School, Universitas Padjadjaran, West Java, Indonesia.
- Email: *susanti.withaningsih@unpad.ac.id*
- ORCID: 0000-0002-5893-0222
- Web of Science ResearcherID: AAB-6734-2021
- Scopus Author ID: 57195276031
- Homepage: https://pasca.unpad.ac.id/en/about-graduate-school/organizational-structure/

Parikesit, P., Ph.D., Professor, Department of Biology, Faculty of Mathematics and Natural Sciences, Universitas Padjadjaran, Sumedang, West Java, Indonesia.
- Email: *parikesit@unpad.ac.id*
- ORCID: 0000-0001-8214-7126
- Web of Science ResearcherID: AAC-9331-2021
- Scopus Author ID: 55934491300
Homepage: https://www.biologi-unpad.ac.id/dosen/